


Article

New Butenolides and Cyclopentenones from Saline Soil-Derived Fungus *Aspergillus Sclerotiorum*

Li-Ying Ma ¹, Huai-Bin Zhang ¹, Hui-Hui Kang ¹, Mei-Jia Zhong ¹, De-Sheng Liu ^{1,*}, Hong Ren ² and Wei-Zhong Liu ^{1,*} ¹ College of Pharmacy, Binzhou Medical University, Yantai 264003, China² Beijing Higher Institution Engineering Research Center of Food Additives and Ingredients, Beijing Key Laboratory of Flavor Chemistry, Beijing Laboratory for Food Quality and Safety, Beijing Technology and Business University, Beijing 100048, China* Correspondence: desheng_liu@sina.com (D.-S.L.); lwz1963@163.com (W.-Z.L.);
Tel.: +86-535-691-3205 (W.-Z.L.)

Received: 3 July 2019; Accepted: 20 July 2019; Published: 21 July 2019



Abstract: Three new γ -hydroxyl butenolides (**1–3**), a pair of new enantiomeric spiro-butenolides (**4a** and **4b**), a pair of enantiomeric cyclopentenones (**5a** new and **5b** new natural), and six known compounds (**6–11**), were isolated from *Aspergillus sclerotiorum*. Their structures were established by spectroscopic data and electronic circular dichroism (ECD) spectra. Two pairs of enantiomers [(+)/(–)-**6c** and (+)/(–)-**6d**] obtained from the reaction of **6** with acetyl chloride (AcCl) confirmed that **6** was a mixture of two pairs of enantiomers. In addition, the X-ray data confirmed that **7** was also a racemate. The new metabolites (**1–5**) were evaluated for their inhibitory activity against cancer and non-cancer cell lines. As a result, compound **1** exhibited moderate cytotoxicity to HL60 and A549 with IC₅₀ values of 6.5 and 8.9 μ M, respectively, and weak potency to HL-7702 with IC₅₀ values of 17.6 μ M. Furthermore, compounds **1–9** were screened for their antimicrobial activity using the micro-broth dilution method. MIC values of 200 μ g/mL were obtained for compounds **2** and **3** towards *Staphylococcus aureus* and *Escherichia coli*, while compound **8** exhibited a MIC of 50 μ g/mL towards *Candida albicans*.

Keywords: *Aspergillus sclerotiorum*; γ -hydroxyl butenolides; cyclopentenones; enantiomer; cytotoxicity; antimicrobial activity

1. Introduction

Aspergillus sclerotiorum widely distributes in various environments such as marine samples, soil, sea-salt field, and rotting apples, and produces a series of bioactive metabolites. Representatives include asterriquinones [1], aspochracin derivative [2], lovastatin analogues [3], butenolides [4], cyclopeptides [5–7], sclerotiamide [8], hydroxamic acids [9], and ochratoxin [10]. In addition, co-incubation of this strain with *Penicillium citrinum* resulted in the production of furanone derivatives and alkaloids [11].

The Yellow River Delta is formed mainly by the deposition of sand and mud carried by the Yellow River, which is the world's youngest wetland ecosystem [12]. High evaporation and tidal intrusion heavily salinizes and alkalizes the soil, half of which is barren and not suitable for the growth of crops [13,14]. The saline soil is typically characterized by poor nutrient and high salinity, which endows the microorganism special biosynthetic pathways during the evolutionary process to produce structurally novel and biologically active secondary metabolites. Up to now, only a few research papers have been carried out on the fungi from this unique environment [15]. In our continuation of investigation on the saline soil-derived fungi from the Yellow River Delta, dozens of natural products (NPs) with multifarious structural features and a wide range of biological activities

were obtained [16,17]. As part of our ongoing efforts in seeking for new bioactive NPs, *A. sclerotiorum* JH42 with antimicrobial activity was isolated from saline soil, and subjected to chemical exploration, which led to the achievement of six new (**1–3**, **4a**, **4b**, and **5a**), a new natural (**5b**), and six known (**6–11**) compounds (Figure 1). Additionally, the isolated γ -hydroxyl butenolides in the current work were all proved to undergo tautomerism at C-4 based on the analyses of physicochemical properties, calculated ECD data, and X-ray diffraction. Herein, details of the isolation, structure elucidation, acetylation, cytotoxic, and antimicrobial activities of these compounds are reported.

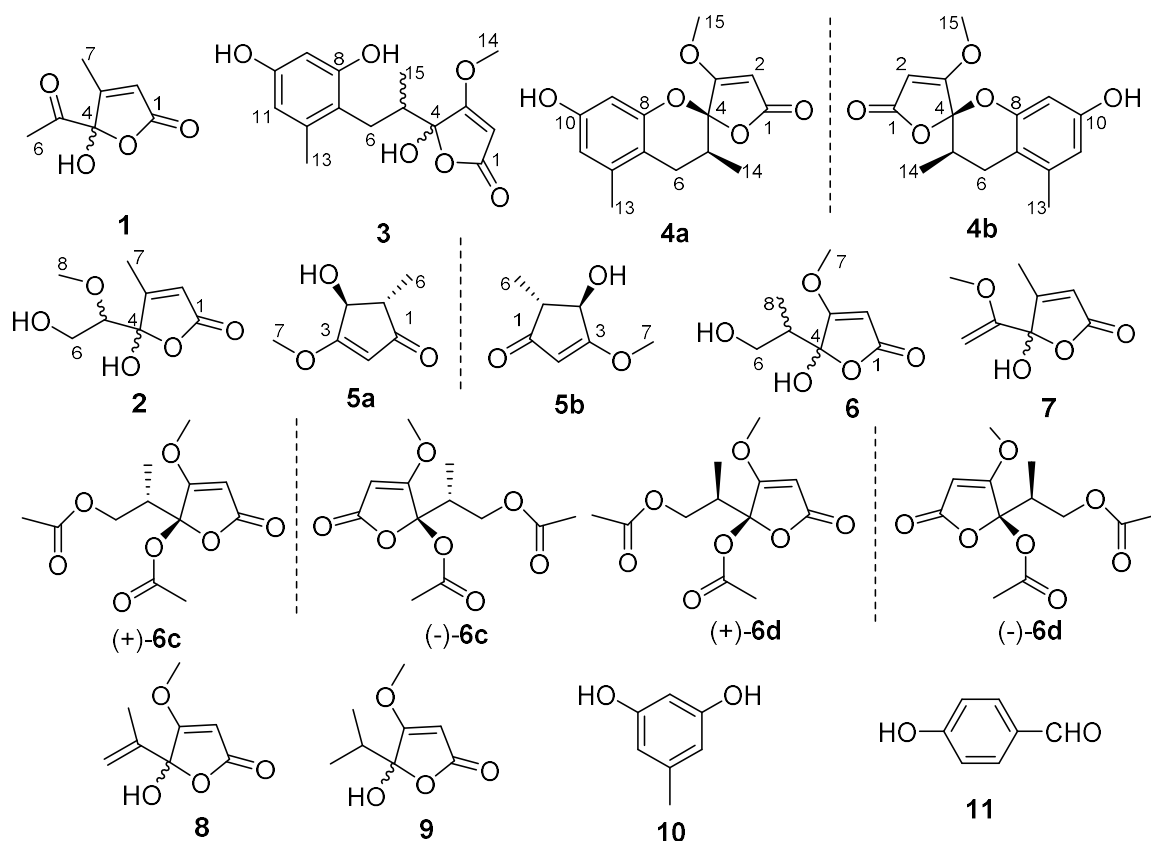


Figure 1. Structures of Compounds **1–3**, **4a**, **4b**, **5a**, **5b**, **6–11**, (+)/(–)-**6c** and (+)/(–)-**6d**.

2. Results

Compound **1** was obtained as an optically inactive colorless oil with the molecular formula of $C_7H_8O_4$ as determined by the deprotonated-ion HRESIMS at m/z 155.0339 $[M - H]^-$ (calcd for $C_7H_7O_4$, 155.0344). Its IR spectrum indicated the presence of hydroxyl (3374 cm^{-1}), keto carbonyl (1755 cm^{-1}), α,β -unsaturated lactone groups ($1731, 1652\text{ cm}^{-1}$) [18]. The ^1H NMR spectrum (Table 1) in $\text{DMSO-}d_6$ showed two singlet methyls at δ_{H} 2.25 and 1.96, a singlet olefinic proton at δ_{H} 6.18, and a hydroxyl group at δ_{H} 8.50. Its ^{13}C NMR spectrum revealed seven carbon resonances, corresponding to a keto carbonyl (δ_{C} 201.5), four diagnostic carbon signals (δ_{C} 170.2, 165.7, 118.9 and 105.7) for a γ -hydroxyl butenolide moiety [4], and two methyl groups (δ_{C} 24.7 and 12.7) (Table 1). The gross structure of **1** was unambiguously established by the HMBC correlations from H-2 to C-1, C-3 and C-4, from H-6 to C-4 and C-5, and from H-7 to C-1, C-3 and C-4 (Figure 2). It was a mixture of inseparable enantiomers, which mutually transformed through the γ -keto-acid form as existence in penicillic acid [19].

Compound **2** was also isolated as an optically inactive colorless oil with the molecular formula of $C_8H_{12}O_5$ as elucidated by the HRESIMS m/z 187.0610 $[M - H]^-$ (calcd for $C_8H_{11}O_5$, 187.0601). The IR absorption bands at $3373, 1739$ and 1652 cm^{-1} suggested the presence of hydroxyl, α,β -unsaturated lactone groups. The ^1H NMR spectrum in $\text{MeOH-}d_4$ displayed signals for a singlet olefinic proton at δ_{H} 5.86, an oxymethine at δ_{H} 3.56 (dd, $J = 7.0, 3.2\text{ Hz}$), a diastereotopic methylene at δ_{H} 3.90 (m) and

3.66 (dd, $J = 11.7, 7.0$ Hz), a methoxyl at δ_{H} 3.50 (s) and a methyl at δ_{H} 2.09 (Table 1). The ^{13}C NMR spectrum (Table 1), with the help of DEPT and HSQC data, showed the presence of two methyls (one oxygenated), an oxymethylene, an olefinic and an oxymethine, a hemiketal carbon (δ_{C} 110.1), and two quaternary carbons (δ_{C} 172.9 and 168.7). The above data indicated **2** was also a γ -hydroxyl butenolide as **1**. The main differences were the appearances of an oxygenated methyl, an oxymethylene and an oxymethine, together with the disappearances of a carbonyl and a methyl. The planar structure and the assignments of the NMR data were completed by the HMBC correlations (Figure 2). Since no optical rotation and no CD absorption exhibited, compound **2** was also an inseparable racemic mixture.

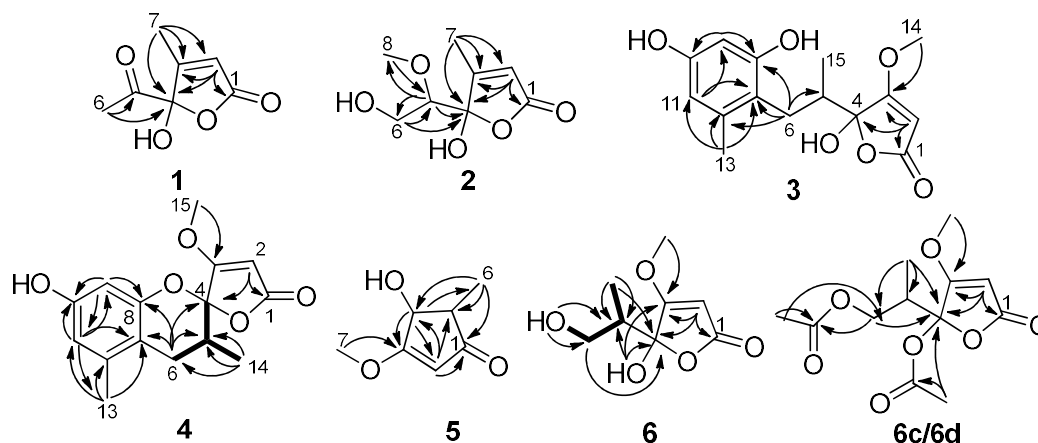


Figure 2. Key COSY and HMBC correlations of **1**–**6**, **6c** and **6d**.

Table 1. ^1H (400 MHz) and ^{13}C (100 MHz) NMR data for **1**, **2** and **5** [δ_{H} , mult (J in Hz)].

Position	1 ^a		2 ^b		5 ^b	
	δ_{C}	δ_{H}	δ_{C}	δ_{H}	δ_{C}	δ_{H}
1	170.2, C		172.9, C		203.8, C	
2	118.9, C	6.18, s	119.5, CH	5.86, br s	127.6, CH	6.37, d (2.6)
3	165.7, C		168.7, C		158.2, C	
4	105.7, C		110.1, C		74.2, CH	4.37, dd (2.6, 1.6)
5	201.5, C		84.2, CH	3.56, dd (7.0, 3.2)	51.1, CH	2.20, dq (7.5, 1.6)
6	24.7, CH	2.25, s	62.4, CH ₂	3.90, m; 3.66, dd (11.7, 7.0)	13.3, CH ₃	1.20, d (7.5)
7	12.7, CH	1.96, s	13.4, CH ₃	2.09, br s	57.7, CH ₃	3.75, s
8			60.6, CH ₃	3.50, s		
OH		8.50, s				

^a NMR spectra obtained in DMSO- d_6 ; ^b NMR spectra obtained in MeOH- d_4 .

Compound **3** was a colorless solid with zero optical rotation. Its HRESIMS at m/z 293.1021 [$\text{M} - \text{H}]^-$ (calcd for $\text{C}_{15}\text{H}_{17}\text{O}_6$, 293.1020) gave the molecular formula of $\text{C}_{15}\text{H}_{18}\text{O}_6$. The ^1H NMR spectrum displayed signals for two meta-coupled aromatic protons at δ_{H} 6.38 and 6.20 (d, $J = 1.6$ Hz, each), one isolated olefinic proton at δ_{H} 5.20, a set of nonequivalent methylene protons at δ_{H} 2.58 and 2.08, one methine at δ_{H} 2.35 (m), one methoxyl at δ_{H} 3.94 and two methyl protons at δ_{H} 2.19 and 0.86 (Table 2). The ^{13}C NMR spectrum displayed fifteen resonance signals (Table 2). The carbon signals at δ_{C} 180.9, 170.7, 106.3, 90.2 and 60.0 showed the representative resonances for a γ -hydroxyl- β -methoxyl butenolide moiety as in dihydropenicillic acid [20], which was also isolated in the current report. Obviously, two aromatic methines and four aromatic quaternary carbons constructed a tetrasubstituted phenyl ring, and the linkages of substituents were completed by the HMBC correlations (Figure 2). The splitting behaviors of methylene at δ_{H} 2.58 (dd, $J = 13.6, 11.2$ Hz) and 2.08 (disturbed by the signals of solvent), methine at δ_{H} 2.35 (m) and methyl at δ_{H} 0.86 (br s) completed the structure of **3**. The weak carbon signals of C-4, C-6, C-7, and C-14, together with the broad singlet of H-14 (should be doublet)

(Figure S15 and S16), implied that the C-4 anomers mutually transformed in solution. Owing to no optical rotation and no CD absorption displayed, **3** existed as an inseparable racemic mixture.

Table 2. ^1H (400 MHz) and ^{13}C (100 MHz) NMR data for **3** and **4** in acetone- d_6 .

Position	3		4	
	δ_{C}	δ_{H} , mult (J in Hz)	δ_{C}	δ_{H} , mult (J in Hz)
1	170.7, C		169.9, C	
2	90.2, CH	5.20, s	91.2, CH	5.44, s
3	180.9, C		178.4, C	
4	106.3, C		104.2, C	
5	39.7, CH	2.35, m	31.4, CH	2.35 ^c
6	26.4, CH ₂	2.58, dd (13.6, 11.2); 2.08 ^a	27.1, CH ₂	2.77, m; 2.35 ^c
7	117.1, C		112.2, C	
8	157.3, C		153.2, C	
9	101.2, CH	6.38, d (1.6)	101.8, CH	6.18, d (2.2)
10	156.8, C		157.3, C	
11	109.7, CH	6.20, d (1.6)	111.9, CH	6.38, d (2.2)
12	139.4, C		138.6, C	
13	20.1, CH ₃	2.19, s	19.1, CH ₃	2.16, s
14	60.0, CH ₃	3.94, s	60.7, CH ₃	4.07, s
15	13.3, CH ₃	0.86, br s ^b	15.1, CH ₃	0.99, d (5.6)

^a Disturbed by solvent; ^b Caused by the mutually transformed anomers of C-4 in solution; ^c Overlapping signals.

Compound **4** was afforded as an optically inactive colorless solid. The HRESIMS m/z 277.1071 $[\text{M} + \text{H}]^+$ gave a molecular formula of $\text{C}_{15}\text{H}_{16}\text{O}_5$, which was one H_2O unit less than that of **3**. Its ^1H and ^{13}C NMR data were similar to those of **3**, except for the chemical shifts of C-4, C/H-5, C/H-6, C-7 and C-8 (Table 2). The above information, especially the chemical shift of C-8 (δ_{C} 153.2), implied that 8-OH and 4-OH in **3** should be dehydrated into an ether linkage in **4**. The 2D NMR spectra (Figure 2) established its planar structure, which was different from aspergispikoketal in the locations of the substituents at benzyl moiety [21], as proved by the HMBC correlations from H-6 to C-7 and C-8, from H-9 to C-8, C-10 and C-11, from H-11 to C-7, C-9, C-10 and C-13, and from H-13 to C-7, C-11 and C-12. In view of no optical activity and ECD absorption, **4** was a racemate and separated into (+)-**4** and (−)-**4** using high performance liquid chromatography (HPLC) on a chiral column. Their absolute configurations were determined according to the experimental and calculated ECD data (Figure 3). Based on the optimized structures, the ECD calculation was conducted using time-dependent density functional theory (TD-DFT) at BP86/6-311G (d,p) for four isomers of **4** (Attachment S1). Then the absolute configurations of (+)-**4** and (−)-**4** were determined to be (4*S*,5*R*)-**4b** and (4*R*,5*S*)-**4a**, respectively.

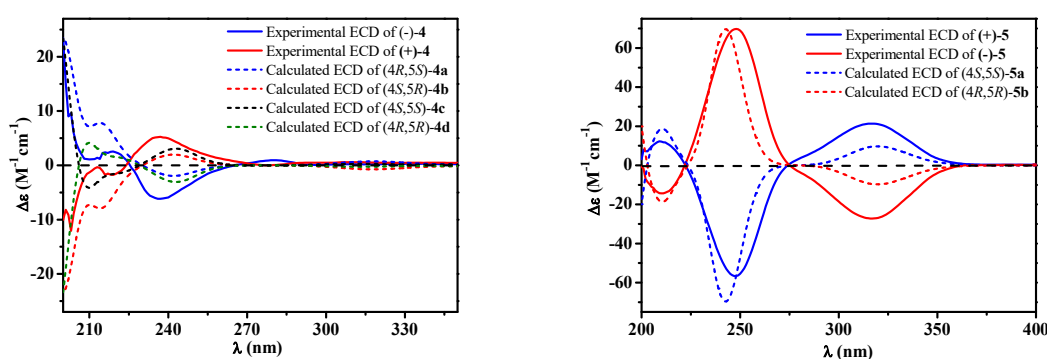


Figure 3. Experimental [(+)/(−)-**4**, (+)/(−)-**5**] and calculated [**4a**, **4b**, **4c**, **4d**, **5a** and **5b**] electronic circular dichroism (ECD) spectra.

Compound **5**, a colorless solid with zero optical rotation, was assigned the molecular formula of $C_7H_{10}O_3$ on the basis of its positive HRESIMS at m/z 143.0704 $[M + H]^+$ (calcd for $C_7H_{11}O_3$, 143.0703). The 1H NMR spectrum showed an olefinic proton at δ_H 6.37 (d, $J = 2.6$ Hz), a oxymethine at δ_H 4.37 (dd $J = 2.6, 1.6$ Hz), a methine at δ_H 2.20 (qd, $J = 7.5, 1.6$ Hz), a methoxyl at δ_H 3.75 (s) and a doublet methyl at δ_H 1.20 ($J = 7.5$ Hz) (Table 1). The ^{13}C NMR spectrum displayed seven carbon signals including a keto carbonyl, two olefinic and four aliphatic carbons (Table 1). The planar structure of **5** was confirmed by the HMBC correlations (Figure 2). In the NOE difference experiment, the signal of H-2 was enhanced when H-6 was irradiated, so H-2 and H-3 were in the opposite directions, which was further confirmed by the small coupling constant ($J = 1.6$ Hz). Compound **5** was subjected to chiral HPLC and separated into (+)-**5** and (–)-**5**. According to the calculated and experimental ECD data (Figure 3), their absolute configurations were determined to be 2*S*,3*S* and 2*R*,3*R* for **5a** and **5b**, respectively. **5b** had been reported as a synthetic intermediate without ^{13}C NMR, ECD and specific rotation data reported [22]. Therefore, **5a** was a new compound, while **5b** was a new natural product.

Compound **6** was obtained as colorless blocks with the molecular formula of $C_8H_{12}O_5$ on the basis of its negative HRESIMS. Some articles reported its structure with a set of 1H and ^{13}C NMR data [4,23], but the compound obtained in our project showed two sets of 1H and ^{13}C NMR data (**6a** and **6b**) (Table 3) with the ratio of about 1:1 in DMSO- d_6 , about 2:1 in acetone- d_6 (only 1H NMR spectrum measured, Figure S42), about 1.4:1 in MeOH- d_4 . Additionally, only H-6, H-8, and C-5 exhibited two sets of NMR signals, and signals of C-3 and C-4 were too weak to be observed in MeOH- d_4 (Figure S43 and S44). The above phenomena suggested **6** was a mixture of two pairs of racemates, and the proportion of anomers of C-4 changed with solvents (Figure 4). The structures and the assignments of the 1H and ^{13}C NMR data of **6a** and **6b** in DMSO- d_6 were completed by 2D NMR spectra (Figure 2).

Table 3. 1H (400 MHz) and ^{13}C (100 MHz) NMR data for **6a** and **6b** in DMSO- d_6 .

Position	6a		6b	
	δ_C	δ_H , mult (J in Hz)	δ_C	δ_H , mult (J in Hz)
1	169.9, C		170.0, C	
2	89.3, CH	5.28, s	89.4, CH	5.23, s
3	179.9, C		179.5, C	
4	103.7, C		104.3, C	
5	41.6, CH	2.02, m	40.5, CH	1.99, m
6	61.4, CH ₂	3.39, dt (10.5, 4.6); 3.09, m	61.1, CH ₂	3.76, dt (10.5, 5.0); 3.19, m
7	59.6, CH ₃	3.83, s	59.7, CH ₃	3.86, s
8	11.0, CH ₃	0.93, d (6.9)	11.3, CH ₃	0.78, d (6.9)
4-OH		7.44, s		7.52, s
6-OH		4.51, t (5.3)		4.68, t (5.3)

In order to explore the case, compound **6** was reacted with AcCl leading to the production of **6c** and **6d** with optical inactivity (Figure 4). Their molecular formulae of $C_{12}H_{16}O_7$ were obtained on the basis of their HRESIMS. And their planar structures were constructed by the 1H and ^{13}C NMR (Table 4) and HMBC spectra (Figure 4). The single crystal X-ray diffraction using Cu $K\alpha$ radiation showed **6c** to be a centrosymmetric space group $P2_1/C$ with 4*S*,5*R* and 4*R*,5*S* configurations (Figure 5), so (±)-**6d** should be the 4*S*,5*S* and 4*R*,5*R* configurations. Then they were subjected to chiral HPLC and isolated into (+)/(–)-**6c** and (+)/(–)-**6d**, respectively. The calculated and experimental ECD data (Figure 6) proved the absolute configurations of (+)-**6c** and (–)-**6c** to be the respective 4*R*,5*S* and 4*S*,5*R*. Considering their ECD absorptions mainly resulted from C-4 chiral center, the same ECD data of (+)-**6c** and (+)-**6d**, and (–)-**6c** and (–)-**6d** to the mirror images, implied that (+)-**6d** and (–)-**6d** had 4*R*,5*R* and 4*S*,5*S* configurations, respectively. The δ values of C-1, C-2 and C-4 in **6c** were slightly larger than those in **6d** with C-3 and C-5 to the contrary (Table 4), and the same behaviors were also observed in **6b** and **6a** (Table 3), so (±)-**6c** and (±)-**6d** should derive from **6b** and **6a**, separately. Consequently, **6b** should be a racemate with the configurations of 4*S*,5*R* and 4*R*,5*S*, **6a** be 4*S*,5*S* and 4*R*,5*R*.

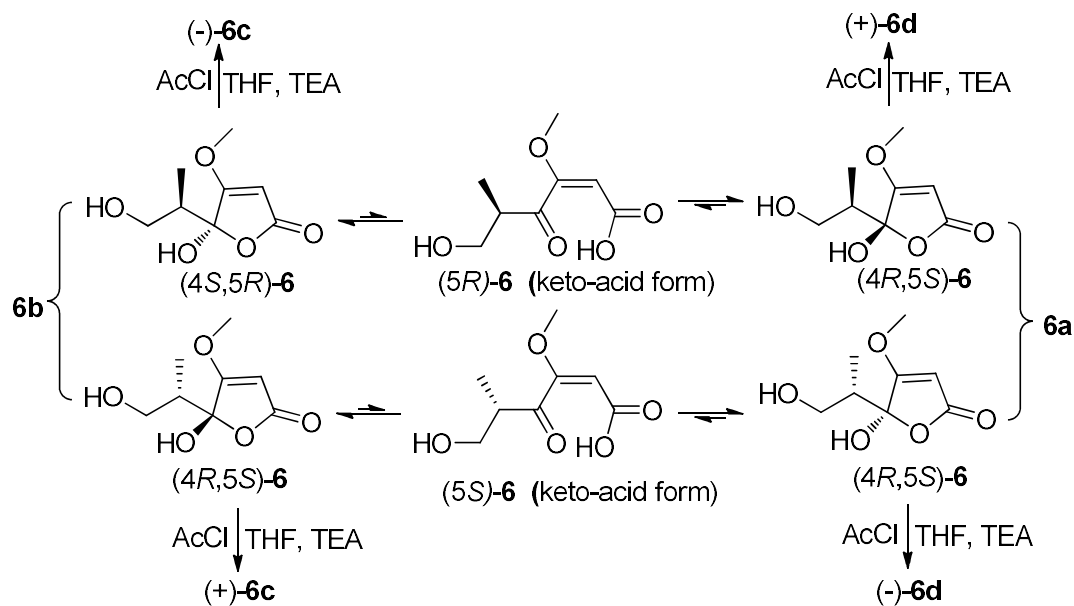


Figure 4. Tautomeric forms (γ -keto-acids and γ -hydroxyl butenolides) of **6**, and the reaction of **6** with AcCl.

Table 4. ^1H (400 MHz) and ^{13}C (100 MHz) NMR data for (\pm)-**6c** and (\pm)-**6d** in $\text{DMSO-}d_6$.

Position	(\pm)- 6c		(\pm)- 6d	
	δ_{C}	δ_{H} , mult (J in Hz)	δ_{C}	δ_{H} , mult (J in Hz)
1	168.6, C		168.5, C	
2	91.2, CH	5.66, s	91.1, CH	5.64, s
3	177.1, C		177.3, C	
4	102.4, C		102.2, C	
5	37.8, CH	2.4, m	38.2, CH	2.45, m
6	62.9, CH_2	4.25, dd (11.2, 4.8); 3.96, dd (11.2, 7.0)	63.0, CH_2	3.93, dd (11.6, 6.2); 3.86, dd (11.6, 6.0)
7	60.5, CH_3	3.92, s	60.5, CH_3	3.92, s
8	10.6, CH_3	0.89, d (7.0)	10.8, CH_3	1.03, d (6.9)
9	170.2, C		170.1, C	
10	20.6, CH_3	2.02, s	20.6, CH_3	2.06, s
11	167.9, C		168.0, C	
12	21.1, CH_3	2.08, s	21.1, CH_3	2.08, s

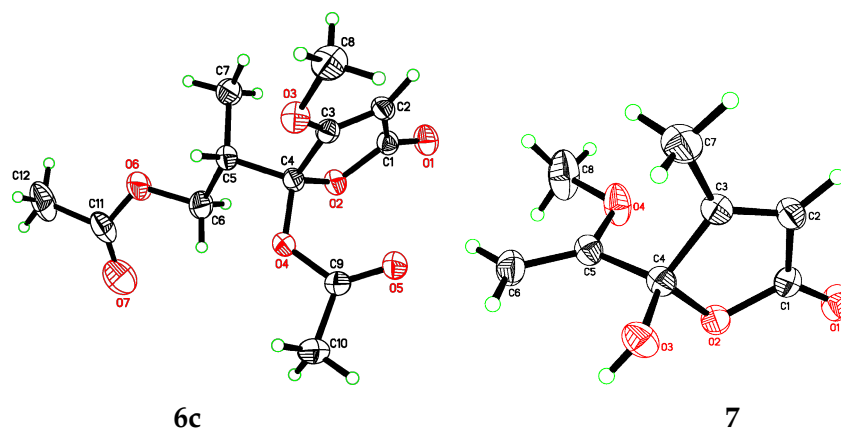


Figure 5. X-ray ORTEP diagrams of **6c** and **7**.

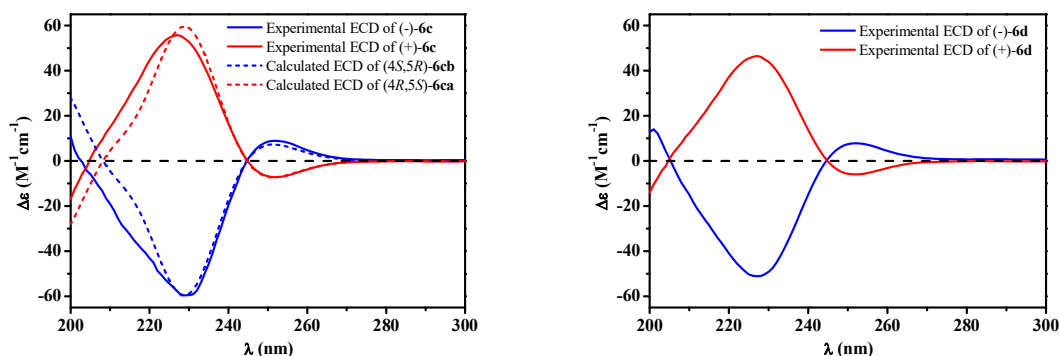


Figure 6. Experimental [(+)/(−)-6c, (+)/(−)-6d] and calculated [(4*S*,5*R*)/(4*R*,5*S*)-6c] ECD spectra.

Compound **7** was isolated as colorless blocks. Its NMR data was almost identical with spersclerotioron G, which was reported as an *S* configuration compound at C-4 chiral center [4]. However, in our report it was optically inactive and of no Cotton effects in its ECD spectrum, therefore it was a racemic mixture, which was confirmed by a centrosymmetric space group $P2_1/n$ in the single crystal X-ray diffraction with Cu $K\alpha$ radiation (Figure 5). Other known compounds were identified as penicillic acid (**8**) [20], dihydropenicillic acid (**9**) [20], orcinol (**10**) [24], and *p*-hydroxyl benzaldehyde (**11**) [25], by comparison of their spectroscopic data with those in the literature.

Compounds **1–5** were preliminarily evaluated for their cytotoxicity against human promyelocytic leukemia (HL60), human lung adenocarcinoma (A549) and human normal liver (HL-7702) cell lines by the MTT method, with doxorubicin as a positive control (IC_{50} : 0.85, 1.5 and 8.3 μ M, respectively). Compound **1** and **3** showed selective cytotoxicity against HL60 (IC_{50} : 6.5 and 12.1 μ M, respectively), A549 (IC_{50} : 8.9 and 16.7 μ M, respectively), and HL-7702 (IC_{50} : 17.6 and 22.8 μ M, respectively) cell lines. The results suggested that compounds **1** and **3** showed stronger cytotoxicity to cancer cells than to non-cancer cell lines. The other compounds were inactive to the tested cell lines ($IC_{50} > 20 \mu$ M).

Meanwhile, the antimicrobial assays of compounds **1–9** were screened against *Staphylococcus aureus* (ATCC 25923), *Escherichia coli* (ATCC 25922) and *Candida albicans* (ATCC 10231). Among them, the known compound **8** showed pronounced antimicrobial activity to the tested organisms, while compounds **2** and **3** displayed weak activity against *S. aureus* and *E. coli* (Table 5).

Table 5. Antimicrobial Activity of Compounds **1–9** (MIC μ g/mL).

	1	2	3	4	5	6	7	8	9	Control
<i>S. aureus</i>	> 400	200	200	> 400	-	> 400	> 400	6.25	> 400	3.12 ^a
<i>E. coli</i>	> 400	200	200	> 400	-	-	-	12.5	-	6.25 ^a
<i>C. albicans</i>	-	-	-	-	-	-	-	50	-	6.25 ^b

^a chloramphenicol; ^b ketoconazole; - no activity.

3. Discussion

A. sclerotiorum JH42 not only produced six new compounds (**1–3**, **4a**, **4b** and **5a**) and a new natural product (**5b**), but also penicillic acid (**8**) with a high yield (59 g in 73 g of the crude extract). Since penicillic acid possessed multiple bioactivities, such as antitumor [19,26–28], antibacterial [4,29], antimalarial [4], phytotoxic [30], antiviral [31], antifungal properties [32], *A. sclerotiorum* JH42 might be employed as a potential producer to provide penicillic acid in industry for the future development and applications.

Additionally, the γ -hydroxyl butenolides (**1–3**, **6–7**) in this study were all proved to be mixtures of enantiomers. The information implied that γ -hydroxyl butenolides usually exist in a mixture of anomers of C-4, which were inseparable because of their mutual transformation through the γ -keto-acid form. The results have guiding significance for the isolation and structure determination of this kind of compounds.

4. Materials and Methods

4.1. General Experimental Procedures

The optical rotations, ultraviolet (UV), IR and ECD spectra were measured on an Autopol V Plus polarimeter (Rudolph Research Analytical, Hackettstown, NJ, USA), a TU-1091 spectrophotometer (Beijing Purkinje General Instrument Co., Beijing, China), Nicolet 6700 spectrophotometer (Thermo Scientific, Waltham, MA, USA) with an attenuated total reflectance (ATR) method, and a Chirascan spectropolarimeter (Applied Photophysics, Leatherhead, United Kingdom), respectively. An Avance 400 (Bruker, Billerica, MA, USA) was used to collect the NMR data. X-ray crystal data were performed on a Bruker Smart 1000 CCD X-ray diffractometer (Bruker Biospin Group, Karlsruhe, Germany). HRESIMS data were acquired on a Q-TOF Ultima GLOBAL GAA076 LC or a 1200RRLC-6520 Accurate-Mass Q-TOF LC/MS mass spectrometer (Agilent, Santa Clara, CA, USA). LC-6AD Liquid Chromatography (Shimadzu, Kyoto, Japan) equipped with an ODS column (HyperClone, 5 μ m ODS C₁₈ 120 Å, 250 \times 10 mm, Phenomenex, 4 mL/min), and a chiral column [ChiralPAK IC, 5 μ m cellulose tri(3,5-dichlorophenyl carbamate), 250 \times 10 mm, Daicel Chiral Technologies Co. LTD. (Shanghai, China)] was used in the HPLC isolation process. The optical density was measured on a Multiskan FC microplate readers (Thermo Fisher Scientific, Shanghai, China). Silica gel (200–300 mesh, Qingdao Marine Chemical Inc., Qingdao, China), reversed-phase C₁₈ silica gel (Pharmacia Fine Chemical Co., Ltd., Uppsala, Sweden) and sephadex LH-20 (Ge Healthcare Bio-Sciences AB, Uppsala, Sweden), were used in column chromatography.

4.2. Fungal Material

A. sclerotiorum JH42 (Genbank accession No. HQ717801) was isolated from the saline soil collected along the coast of Bohai bay in Zhanhua in August 2008. The working strain was identified according to ITS sequence analysis and assigned the accession number JH42. It was preserved in China General Microbiological Culture Collection Center (Depositary Number: CGMCC NO. 13562).

4.3. Fermentation and Extraction

A. sclerotiorum JH42 was cultured on Petri dishes of potato dextrose agar (PDA) at 28 °C for 7 days. A small spoon of spores was transferred into 500-mL conical flasks containing 180 mL culture medium (decoction of 200 g potato, glucose 20 g, maltose 20 g, mannitol 10 g, yeast extract 3 g, KH₂PO₄ 0.5 g, MgSO₄·7H₂O 0.3 g, dissolved in 1 L seawater), and cultured at 28 °C for 9 days on a rotary shaker at 170 rpm. The culture broth (34.5 L) was filtered into filtrate and mycelia. The former was extracted with ethyl acetate, while the latter was extracted with methanol. The methanol solution was concentrated under reduced pressure to yield an aqueous solution, which was then extracted with ethyl acetate. The ethyl acetate extracts were merged and evaporated under reduced pressure to give an extract (73 g).

4.4. Purification

The extract was dissolved in acetone and left for crystallization at room temperature by slow evaporation of the solvent to obtain **8** (18.0 g). Then the residue was performed on a silica gel column chromatography with a step gradient of petroleum ether/ethyl acetate (from 1:0 to 0:1, *v/v*) to afford ten fractions (Fr.s 1–10). Fr. 7 (3.6 g) was separated into seven subfractions (Fr.s 7.1–7.7) by an ODS column eluting with MeOH/H₂O gradient (from 20:80 to 100:0, *v/v*). Fr. 7.2 (0.2 g) was purified by semipreparative HPLC on an ODS column eluting with 15% MeOH to yield **1** (25.2 mg, *t*_R 7.9 min) and **2** (14.2 mg, *t*_R 5.6 min). Fr. 4 (1.1 g) was chromatographed on a Sephadex LH-20 column (MeOH) and then purified by HPLC (60% MeOH) to yield **3** (38.0 mg, *t*_R 22.1 min). Fr. 7.6 (0.1 g) was purified by HPLC (40% MeOH) on an ODS column to yield **4** (12.0 mg, *t*_R 26.8 min), which was further separated by HPLC on a chiral column (n-hexane/isopropanol, 60:40, *v/v*, 2.0 mL/min) to give **4a** (1.8 mg, *t*_R 17.3 min) and **4b** (1.7 mg, *t*_R 41.5 min). Fr. 7.3 (0.1 g) was separated by HPLC (15% MeOH) to afford **5**

(14.6 mg, t_R 12.2 min), which was further separated by HPLC on a chiral column (n-hexane/isopropanol, 60:40, v/v , 2.0 mL/min) to give **5a** (2.5 mg, t_R 28.6 min) and **5b** (3.3 mg, t_R 21.3 min). Fr. 6 (1.3 g) was chromatographed on a silica gel column using chloroform/methanol (30:1, v/v) to obtain **6** (0.63 g). Fr. 5 (44.0 g) was crystallized in acetone to give **8** (41.0 g) again, and then the residue was isolated by HPLC (25% MeOH) to yield **7** (16.0 mg, t_R 13.8 min) and **9** (27.0 mg, t_R 20.3 min). Fr. 8 (0.35 g) was purified by HPLC (15% MeOH) to yield **10** (13.8 mg, t_R 27.2 min) and **11** (9.8 mg, t_R 21.2 min).

Aspersclerolide A (**1**): colorless oil (MeOH); UV (MeOH) λ_{max} (log ϵ): 210 (3.94) nm; IR (ATR) ν_{max} 3374, 1755, 1731, 1652, 1435, 1382, 1360, 1302, 1202, 1149, 1018, 912, 857, 765 cm^{-1} ; 1H and ^{13}C NMR data: see Table 1; HRESIMS m/z 155.0339 [M – H] $^-$ (calcd for $C_7H_7O_4$, 155.0344).

Aspersclerolide B (**2**): colorless oil (MeOH); UV (MeOH) λ_{max} (log ϵ): 206 (3.88) nm; IR (ATR) ν_{max} 3373, 2943, 1739, 1652, 1438, 1380, 1185, 1114, 1037, 922, 853, 697 cm^{-1} ; 1H and ^{13}C NMR data: see Table 1; HRESIMS m/z 187.0610 [M – H] $^-$ (calcd for $C_8H_{11}O_5$, 187.0601).

Aspersclerolide C (**3**): colorless solid (MeOH); UV (MeOH) λ_{max} (log ϵ): 282 (3.35), 221 (4.14), 205 (4.46) nm; IR (ATR) ν_{max} 3369, 3251, 1742, 1706, 1630, 1593, 1511, 1456, 1342, 1293, 1267, 1222, 1142, 1095, 985, 911, 806, 780 cm^{-1} ; 1H and ^{13}C NMR data: see Table 2; HRESIMS m/z 293.1021 [M – H] $^-$ (calcd for $C_{15}H_{17}O_6$, 293.1020).

(\pm)-Aspersclerolide D (**4**): colorless solid (MeOH); UV (MeOH) λ_{max} (log ϵ): 279 (3.51), 221 (4.13), 210 (4.11) nm; IR (ATR) ν_{max} 3326, 1737, 1679, 1639, 1626, 1594, 1501, 1451, 1373, 1342, 1266, 1173, 1061, 993, 926, 802, 776 cm^{-1} ; 1H and ^{13}C NMR data: see Table 2; HRESIMS m/z 277.1071 [M + H] $^+$ (calcd for $C_{15}H_{17}O_5$, 277.1071).

(–)-Aspersclerolide D (**4a**): colorless solid (MeOH); $[\alpha]_D^{20}$ –39.8 (c 0.090, MeOH); ECD (MeOH) λ_{max} ($\Delta\epsilon$) 280 (+0.95), 237 (–6.16), 219 (+2.54) nm.

(+)-Aspersclerolide D (**4b**): colorless solid (MeOH); $[\alpha]_D^{20}$ +36.9 (c 0.084, MeOH); ECD (MeOH) λ_{max} ($\Delta\epsilon$) 278 (–0.003), 237 (+5.24), 219 (–1.75) nm.

(\pm)-4-hydroxy-3-methoxy-5-methyl-2-cyclopentenone (**5**): colorless solid (MeOH); UV (MeOH) λ_{max} (log ϵ): 246 (3.75) nm; IR (ATR) ν_{max} 3405, 2943, 1712, 1627, 1456, 1316, 1252, 1130, 1074, 1006, 937, 888, 844, 794 cm^{-1} ; 1H and ^{13}C NMR data: see Table 1; HRESIMS m/z 143.0704 [M – H] $^-$ (calcd for $C_7H_{11}O_3$, 143.0703).

(+)-(4*S*,5*S*)-4-hydroxy-3-methoxy-5-methyl-2-cyclopentenone (**5a**): colorless solid (MeOH); $[\alpha]_D^{20}$ +11.11 (c 0.13, MeOH); ECD (MeOH) λ_{max} ($\Delta\epsilon$) 317 (+21.36), 247 (–56.64), 209 (+12.29) nm.

(–)-(4*R*,5*R*)-4-hydroxy-3-methoxy-5-methyl-2-cyclopentenone (**5b**): colorless solid (MeOH); $[\alpha]_D^{20}$ –12.65 (c 0.17, MeOH); ECD (MeOH) λ_{max} ($\Delta\epsilon$) 317 (–27.20), 248 (+69.81), 210 (–14.32) nm.

6-hydroxyl dihydropenicillic acid (**6**): colorless blocks (MeOH); UV (MeOH) λ_{max} (log ϵ): 223 (3.98) nm; IR (ATR) ν_{max} 3309, 3112, 1742, 1709, 1622, 1449, 1414, 1356, 1294, 1268, 1223, 1167, 1094, 1038, 1021, 986, 953, 935, 899, 817, 783, 675 cm^{-1} ; 1H and ^{13}C NMR data: see Table 3; HRESIMS m/z 187.0615 [M – H] $^-$ (calcd for $C_8H_{11}O_5$, 187.0606).

(\pm)-**6c**: colorless blocks (MeOH); 1H and ^{13}C NMR data: see Table 4; HRESIMS m/z 295.0809 [M + Na] $^+$ (calcd for $C_{12}H_{16}O_7Na$, 295.0788).

(+)-**6c**: colorless solid (MeOH); $[\alpha]_D^{20}$ +43.90 (c 0.04, MeOH); ECD (MeOH) λ_{max} ($\Delta\epsilon$) 252 (–7.22), 227 (+55.82) nm.

(–)-**6c**: colorless solid (MeOH); $[\alpha]_D^{20}$ –46.15 (c 0.03, MeOH); ECD (MeOH) λ_{max} ($\Delta\epsilon$) nm; 252 (+8.92), 229 (–59.62) nm.

(\pm)-**6d**: colorless solid (MeOH); 1H and ^{13}C NMR data: see Table 4; HRESIMS m/z 295.0780 [M + Na] $^+$ (calcd for $C_{12}H_{16}O_7Na$, 295.0788).

(+)-**6d**: colorless solid (MeOH); $[\alpha]_D^{20}$ +78.57 (c 0.08, MeOH); ECD (MeOH) λ_{max} ($\Delta\epsilon$) 252 (–6.01), 227 (+46.51) nm.

(–)-**6d**: colorless solid (MeOH); $[\alpha]_D^{20}$ –80.00 (c 0.06, MeOH); ECD (MeOH) λ_{max} ($\Delta\epsilon$) 252 (+7.82), 227 (–51.14) nm.

X-ray Single-Crystal Structure Determinations of **6c** and **7**. Colorless crystals of **6c** and **7** were obtained from MeOH. Their structures were solved by direct methods using the SHELXTL software

package and refined by least squares minimization. The crystallographic data for **6c** (deposition number: CCDC 1912596) and **7** (deposition number: CCDC 1912598) have been deposited in the Cambridge Crystallographic Data Centre. These data can be obtained free of charge from the Cambridge Crystallographic Data Centre via www.ccdc.cam.ac.uk/data_request/cif.

Crystal data for **6c**. $C_{12}H_{16}O_7$, $M_r = 272.25$, Monoclinic, space group $P2_1/c$, unit cell dimensions $a = 8.6937(3) \text{ \AA}$, $b = 22.0810(5) \text{ \AA}$, $c = 7.9551(2) \text{ \AA}$, $V = 1392.71(7) \text{ \AA}^3$, $Z = 4$, $D_{\text{calcd}} = 1.298 \text{ g/cm}^3$, $F(000) = 576$. $\alpha = \gamma = 90.00$, $\beta = 114.218(4)$; A total of 2427 unique reflections were collected, with 2123 reflections greater than $I \geq 2\sigma(I)$ ($R_{\text{int}} = 0.0165$). The structure was solved by direct methods and refined by full-matrix least-squares on F^2 , with anisotropic displacement parameters for non-hydrogen atoms at final R indices [$I > 2\sigma(I)$], $R_1 = 0.0445$, $wR_2 = 0.1199$; R indices (all data), $R_1 = 0.0503$, $wR_2 = 0.1249$.

Crystal data for **7**. $C_8H_{10}O_4$, $M_r = 170.16$, Monoclinic, space group $P2_1/n$, unit cell dimensions $a = 7.6359(3) \text{ \AA}$, $b = 13.2597(4) \text{ \AA}$, $c = 8.5653(3) \text{ \AA}$, $V = 852.49(5) \text{ \AA}^3$, $Z = 4$, $D_{\text{calcd}} = 1.326 \text{ g/cm}^3$, $F(000) = 360$. $\alpha = \gamma = 90.00$, $\beta = 100.581(2)$; A total of 1482 unique reflections were collected, with 1394 reflections greater than $I \geq 2\sigma(I)$ ($R_{\text{int}} = 0.0185$). The structure was solved by direct methods and refined by full-matrix least-squares on F^2 , with anisotropic displacement parameters for non-hydrogen atoms at final R indices [$I > 2\sigma(I)$], $R_1 = 0.0414$, $wR_2 = 0.1115$; R indices (all data), $R_1 = 0.0436$, $wR_2 = 0.1130$.

4.5. Preparation and Isolation of (\pm)-**6c** and (\pm)-**6d**

AcCl (41 μ L) was added to a solution of **6** (53 mg) and triethylamine (TEA) (79 μ L) in THF (5 mL). The mixed solution was stirred at room temperature for 2 h. After removal of the solvent under reduced pressure, 5 mL of distilled water was added into the residue and subsequently extracted with ethyl acetate (5 \times 3 mL). The ethyl acetate layer was evaporated under reduced pressure to give a crude product, followed by purification on HPLC with an ODS column (40% MeOH) to give **6c** (11.6 mg, t_R 15.6 min) and **6d** (10.8 mg, t_R 16.6 min). **6c** and **6d** were further separated by HPLC on a chiral column (n-hexane/isopropanol, 60:40, *v/v*, 2.0 mL/min) to give (+)-**6c** (5.2 mg, t_R 68.2 min), (–)-**6c** (4.8 mg, t_R 48.2 min), (+)-**6d** (4.4 mg, t_R 74.2 min) and (–)-**6d** (4.1 mg, t_R 47.5 min), respectively.

4.6. Biological Assay

The cytotoxic activity against HL60, A549 and HL-7702 cell lines was performed by the MTT method as previously described [33].

The antimicrobial assays against *S. aureus*, *E. coli* and *C. albicans* were carried out by the broth microdilution method [34]. The tested organisms were incubated overnight with shaking (200 rpm) in thermostatic oscillation incubator (37 °C) in Mueller Hinton broth (MHB) and liquid Sabourand medium for the bacteria and the fungus, respectively. The microbial inoculum density was adjusted to 1×10^6 cfu/mL with 0.9% saline solution by comparison with a MacFarland standard. The tested substances and positive drugs were dissolved in methanol to an initial concentration of 40 mg/mL. 4 μ L of initial compound solution and 196 μ L of MHB (liquid Sabourand medium for fungus) were added into the first well and mixed evenly. Then 100 μ L of solution from the first hole, along with 2 μ L of methanol and 98 μ L of MHB (liquid Sabourand medium for fungus), were transferred to the second hole, and then shaken up as mixture uniform. The repetitive operation was performed to the eleventh one, from which 100 μ L of solution well was discarded. Then, 100 μ L of microbial suspension was added to the solutions in 96-well to achieve a final volume of 200 μ L and final sample concentrations from 400 to 0.39 μ g/mL. The blank well was also incubated with only medium under the same conditions. All experiments were carried out in triplicate and with chloramphenicol and ketoconazole as the positive controls. Optical density measurement for bacteria and fungus was recorded at 620 nm after incubation at 37 °C for 12 and 24 h, respectively. The minimal inhibitory concentration (MIC) was defined as the concentration at which the growth was inhibited 80% of the tested microorganisms [35].

5. Conclusions

In summary, three new (1–3) and four known (6–9) γ -hydroxyl butenolides, a pair of new enantiomeric spiro-butenolides (4a and 4b), a pair of enantiomeric cyclopentenones (5a new and 5b new natural), along with orcinol (10) and *p*-hydroxyl benzaldehyde (11), were isolated from *A. sclerotiorum* JH42. The acquisition of two pairs of enantiomers [(+)/(–)-6c] and (+)/(–)-6d] by the reaction of 6 with AcCl confirmed that 6 was a mixture of two pairs of enantiomers. In addition, the X-ray diffraction data of 7 revealed it was also a racemic mixture. Compound 1 exhibited moderate cytotoxicity against HL60 and A549 cell lines with IC₅₀ values of 6.5 and 8.9 μ M, respectively. New compounds 2 and 3 showed weak antibacterial activity against *S. aureus* and *E. coli*, while 8 displayed pronounced antimicrobial activity against all the tested organisms.

Supplementary Materials: The following are available online at <http://www.mdpi.com/1420-3049/24/14/2642/s1>, Figure S1: ¹H NMR spectrum (400 MHz) of 1 in DMSO-*d*₆, Figure S2: ¹³C NMR spectrum (100 MHz) of 1 in DMSO-*d*₆, Figure S3: HMBC spectrum of 1 in DMSO-*d*₆, Figure S4: IR spectrum of 1, Figure S5: UV spectrum of 1 in MeOH, Figure S6: HRESIMS of 1, Figure S7: ¹H NMR spectrum (400 MHz) of 2 in MeOH-*d*₄, Figure S8: ¹³C NMR spectrum (100 MHz) of 2 in MeOH-*d*₄, Figure S9: DEPT 135 spectrum of 2 in MeOH-*d*₄, Figure S10: HSQC spectrum of 2 in MeOH-*d*₄, Figure S11: HMBC spectrum of 2 in MeOH-*d*₄, Figure S12: IR spectrum of 2, Figure S13: UV spectrum of 2 in MeOH, Figure S14: HRESIMS of 2, Figure S15: ¹H NMR spectrum (400 MHz) of 3 in acetone-*d*₆, Figure S16: ¹³C NMR spectrum (100 MHz) of 3 in acetone-*d*₆, Figure S17: HMBC spectrum of 3 in acetone-*d*₆, Figure S18: UV spectrum of 3 in MeOH, Figure S19: IR spectrum of 3, Figure S20: HRESIMS of 3, Figure S21: ¹H NMR spectrum (400 MHz) of 4 in acetone-*d*₆, Figure S22: ¹³C NMR spectrum (100 MHz) of 4 in acetone-*d*₆, Figure S23: DEPT spectrum of 4 in acetone-*d*₆, Figure S24: HMQC spectrum of 4 in acetone-*d*₆, Figure S25: ¹H-¹H COSY spectrum of 4 in acetone-*d*₆, Figure S26: HMBC spectrum of 4 in acetone-*d*₆, Figure S27: IR spectrum of 4, Figure S28: UV spectrum of 4 in MeOH, Figure S29: HRESIMS of 4, Figure S30: ¹H NMR spectrum (400 MHz) of 5 in MeOH-*d*₄, Figure S31: ¹³C NMR spectrum (100 MHz) of 5 in MeOH-*d*₄, Figure S32: HMBC spectrum of 5 in MeOH-*d*₄, Figure S33: NOE difference spectrum of 5 in MeOH-*d*₄, Figure S34: IR spectrum of 5, Figure S35: UV spectrum of 5 in MeOH, Figure S36: HRESIMS of 5, Figure S37: ¹H NMR spectrum (400 MHz) of 6 in DMSO-*d*₆, Figure S38: ¹³C NMR spectrum (100 MHz) of 6 in DMSO-*d*₆, Figure S39: ¹H-¹H COSY spectrum of 6 in DMSO-*d*₆, Figure S40: HSQC spectrum of 6 in DMSO-*d*₆, Figure S41: HMBC spectrum of 6 in DMSO-*d*₆, Figure S42: ¹H NMR spectrum (400 MHz) of 6 in acetone-*d*₆, Figure S43: ¹H NMR spectrum (400 MHz) of 6 in MeOH-*d*₄, Figure S44: ¹³C NMR spectrum (100 MHz) of 6 in MeOH-*d*₄, Figure S45: HSQC spectrum of 6 in MeOH-*d*₄, Figure S46: HRESIMS of 6, Figure S47: ¹H NMR spectrum (400 MHz) of 6c in DMSO-*d*₆, Figure S48: ¹³C NMR spectrum (100 MHz) of 6c in DMSO-*d*₆, Figure S49: HMBC spectrum of 6c in DMSO-*d*₆, Figure S50: HRESIMS of 6c, Figure S51: ¹H NMR spectrum (400 MHz) of 6d in DMSO-*d*₆, Figure S52: ¹³C NMR spectrum (100 MHz) of 6d in DMSO-*d*₆, Figure S53: HMBC spectrum of 6d in DMSO-*d*₆, Figure S54: HRESIMS of 6d, Attachment S1: Supporting information for the calculated ECD spectra of compounds 4, 5, and 6c.

Author Contributions: Conceptualization, W.-Z.L. and L.-Y.M.; fermentation, compound purification and bioassay, L.-Y.M., H.-B.Z., H.-H.K., M.-J.Z. and H.R.; structural elucidation, writing and funding acquisition, W.-Z.L.; structural elucidation, review and editing, D.-S.L.

Funding: This research was funded by National Natural Science Foundation of China (No. 31270082) and Natural Science Foundation of Shandong Province, China (No. Y2008B17).

Acknowledgments: *A. sclerotiorum* JH42 was identified by Tianjiao Zhu (Key Laboratory of Marine Drugs, Chinese Ministry of Education; School of Medicine and Pharmacy, Ocean University of China.). We thank Qianqun Gu (Ocean University of China) for giving us the great help and beneficial suggestions in the structure determinations.

Conflicts of Interest: The authors declare no conflict of interest.

References

1. Xu, J.W.; Che, Q.; Zhu, T.J.; Gu, Q.Q.; Li, D.H. The cytotoxics secondary metabolites from South China Sea derived fungus *Aspergillus sclerotoiorum* XJW-56. *Chin. J. Mar. Drugs* **2014**, *33*, 13–18.
2. Motohashi, K.; Inaba, S.; Takagi, M.; Shin-ya, K. JBIR-15, a new aspochracin derivative, isolated from a sponge-derived fungus *Aspergillus sclerotiorum* Huber Sp080903f04. *Biosci. Biotechnol. Biochem.* **2009**, *73*, 1898–1900. [[CrossRef](#)] [[PubMed](#)]
3. Phainuphong, P.; Rukachaisirikul, V.; Saithong, S.; Phongpaichit, S.; Bowornwiriyan, K.; Muanprasat, C.; Srimaroeng, C.; Duangjai, A.; Sakayaroj, J. Lovastatin analogues from the soil-derived fungus *Aspergillus sclerotiorum* PSU-RSPG178. *J. Nat. Prod.* **2016**, *79*, 1500–1507. [[CrossRef](#)] [[PubMed](#)]

4. Phainuphong, P.; Rukachaisirikul, V.; Tadpetch, K.; Sukpondma, Y.; Saithong, S.; Phongpaichit, S.; Preedanon, S.; Sakayaroj, J. γ -Butenolide and furanone derivatives from the soil-derived fungus *Aspergillus sclerotiorum* PSU-RSPG178. *Phytochemistry* **2017**, *137*, 165–173. [[CrossRef](#)] [[PubMed](#)]
5. Zheng, J.; Zhu, H.; Hong, K.; Wang, Y.; Liu, P.; Wang, X.; Peng, X.; Zhu, W. Novel cyclic hexapeptides from marine-derived fungus *Aspergillus sclerotiorum* PT06-1. *Org. Lett.* **2009**, *11*, 5262–5265. [[CrossRef](#)] [[PubMed](#)]
6. Zheng, J.; Xu, Z.; Wang, Y.; Hong, K.; Liu, P.; Zhu, W. Cyclic tripeptides from the halotolerant fungus *Aspergillus sclerotiorum* PT06-1. *J. Nat. Prod.* **2010**, *73*, 1133–1137. [[CrossRef](#)] [[PubMed](#)]
7. Whyte, A.C.; Joshi, B.K.; Gloer, J.B.; Wicklow, D.T.; Dowd, P.F. New cyclic peptide and bisindolyl benzenoid metabolites from the sclerotia of *Aspergillus sclerotiorum*. *J. Nat. Prod.* **2000**, *63*, 1006–1009. [[CrossRef](#)]
8. Whyte, A.C.; Gloer, J.B.; Wicklow, D.T.; Dowd, P.F. Sclerotiamide: a new member of the paraherquamide class with potent antiinsectan activity from the sclerotia of *Aspergillus sclerotiorum*. *J. Nat. Prod.* **1996**, *59*, 1093–1095. [[CrossRef](#)]
9. Micetich, R.G.; Macdona, J.C. Metabolites of *Aspergillus sclerotiorum* Huber. *J. Chem. Soc.* **1964**, 1507–1510. [[CrossRef](#)]
10. Varga, J.; Kevei, E.; Rinyu, E.; Téren, J.; Kozakiewicz, Z. Ochratoxin production by *Aspergillus* species. *Appl. Environ. Microbiol.* **1996**, *62*, 4461–4464. [[CrossRef](#)]
11. Bao, J.; Wang, J.; Zhang, X.-Y.; Nong, X.-H.; Qi, S.-H. New furanone derivatives and alkaloids from the co-culture of marine-derived fungi *Aspergillus sclerotiorum* and *Penicillium citrinum*. *Chem. Biodivers.* **2017**, *14*, e1600327. [[CrossRef](#)] [[PubMed](#)]
12. Song, C.; Liu, G.; Liu, Q. Spatial and environmental effects on plant communities in the Yellow River Delta, Eastern China. *J. For. Res.* **2009**, *20*, 117–122. [[CrossRef](#)]
13. Yu, Y.; Liu, J.; Liu, C.; Zong, S.; Lu, Z. Effect of organic materials on the chemical properties of saline soil in the Yellow River Delta of China. *Front. Earth Sci.* **2015**, *9*, 259–267. [[CrossRef](#)]
14. Guan, Y.; Liu, G.; Wang, J. Saline-alkali land in the Yellow River Delta: amelioration zonation based on GIS. *J. Geogr. Sci.* **2001**, *11*, 313–320.
15. Fu, P.; Liu, P.; Qu, H.; Wang, Y.; Chen, D.; Wang, H.; Li, J.; Zhu, W. α -Pyrone and diketopiperazine derivatives from the marine-derived actinomycete *Nocardioopsis dassonvillei* HR10-5. *J. Nat. Prod.* **2011**, *74*, 2219–2223. [[CrossRef](#)]
16. Liu, W.Z.; Ma, L.Y.; Liu, D.S.; Huang, Y.L.; Wang, C.H.; Shi, S.S.; Pan, X.H.; Song, X.D.; Zhu, R.X. Peniciketals A–C, new spiroketals from saline soil derived *Penicillium raistrichii*. *Org. Lett.* **2014**, *16*, 90–93. [[CrossRef](#)]
17. Kang, H.H.; Zhang, H.B.; Zhong, M.J.; Ma, L.Y.; Liu, D.S.; Liu, W.Z.; Ren, H. Potential antiviral xanthenes from a coastal saline soil fungus *Aspergillus iizukae*. *Mar. Drugs* **2018**, *16*, 449. [[CrossRef](#)]
18. He, J.; Wijeratne, E.M.; Bashyal, B.P.; Zhan, J.; Seliga, C.J.; Liu, M.X.; Pierson, E.E.; Pierson III, L.S.; VanEtten, H.D.; Gunatilaka, A.A. Cytotoxic and other metabolites of *Aspergillus* inhabiting the rhizosphere of Sonoran desert plants. *J. Nat. Prod.* **2004**, *67*, 1985–1991. [[CrossRef](#)]
19. Birkinshaw, J.H.; Oxford, A.E.; Raistrick, H. Studies in the biochemistry of micro-organisms. *Biochem. J.* **1936**, *30*, 394–411. [[CrossRef](#)]
20. Kimura, Y.; Nakahara, S.; Fujioka, S. Aspyrone, a nematocidal compound isolated from the fungus, *Aspergillus melleus*. *Biosci. Biotechnol. Biochem.* **1996**, *60*, 1375–1376. [[CrossRef](#)]
21. Chen, G.; Zhang, L.; Wang, H.; Wang, H.; Wu, H.-H.; Lu, X.; Pei, Y.-H.; Wu, X.; Pan, B.; Hua, H.-M.; et al. A new compound along with seven known compounds from an endophytic fungus *Aspergillus* sp HS-05. *Rec. Nat. Prod.* **2013**, *7*, 320–324.
22. Matoba, K.; Yamazaki, T. Reduction of some vinylogous esters with lithium aluminum hydride. *IV Yakugaku Zasshi.* **1972**, *92*, 213–220. [[CrossRef](#)] [[PubMed](#)]
23. Bao, J.; Zhang, X.-Y.; Yao, Q.-F.; Xu, X.-Y.; Nong, X.-H.; Qi, S.H. Secondary metabolites from the co-culture of gorgonian-associated fungi *Aspergillus sclerotiorum* and *Penicillium citrinum*. *Nat. Prod. Res. Dev.* **2014**, *26*, 1–4.
24. Niu, D.L.; Wang, L.S.; Zhang, Y.J.; Yan, C.R. Chemical constituents of *Acroscyphus sphaerophoroides*. *Plant Sci. J.* **2011**, *29*, 234–237. [[CrossRef](#)]
25. Zhang, D.W.; Dai, S.J.; Liu, W.; Li, G.H. Chemical constituents from the vines of *Pueraria lobata*. *Chin. J. Nat. Med.* **2010**, *8*, 196–198. [[CrossRef](#)]

26. Montenegro, T.G.C.; Rodrigues, F.A.R.; Jimenez, P.C.; Angelim, A.L.; Melo, V.M.M.; Filho, E.R.; Oliveira, M.C.F.; Costa-Lotufo, L.V. Cytotoxic activity of fungal strains isolated from the ascidian *Eudistoma vannamei*. *Chem. Biodivers.* **2012**, *9*, 2203–2209. [[CrossRef](#)] [[PubMed](#)]
27. Vansteelandt, M.; Blanchet, E.; Egorov, M.; Petit, F.; Toupet, L.; Bondon, A.; Monteau, F.; Le Bizec, B.; Thomas, O.P.; Pouchus, Y.F.; et al. Ligerin, an antiproliferative chlorinated sesquiterpenoid from a marine-derived *Penicillium* strain. *J. Nat. Prod.* **2013**, *76*, 297–301. [[CrossRef](#)] [[PubMed](#)]
28. Zheng, C.-J.; Xu, L.-L.; Li, Y.-Y.; Han, T.; Zhang, Q.-Y.; Ming, Q.-L.; Rahman, K.; Qin, L.P. Cytotoxic metabolites from the cultures of endophytic fungi from *Panax ginseng*. *Appl. Microbiol. Biotechnol.* **2013**, *97*, 7617–7625. [[CrossRef](#)]
29. Liu, Y.; Li, X.-M.; Meng, L.-H.; Wang, B.-G. Polyketides from the marine mangrove-derived fungus *Aspergillus ochraceus* MA-15 and their activity against aquatic pathogenic bacteria. *Phytochem. Lett.* **2015**, *12*, 232–236. [[CrossRef](#)]
30. Martínez-Luis, S.; González, M.C.; Ulloa, M.; Mata, R. Phytotoxins from the fungus *Malbranchea aurantiaca*. *Phytochemistry* **2005**, *66*, 1012–1016. [[CrossRef](#)]
31. Suzuki, S.; Kimura, T.; Saito, F.; Ando, K. Antitumor and antiviral properties of penicillic acid. *Agric. Biol. Chem.* **1971**, *35*, 287–290. [[CrossRef](#)]
32. Kang, S.W.; Kim, S.W. New antifungal activity of penicillic acid against *Phytophthora* species. *Biotechnol. Lett.* **2004**, *26*, 695–698. [[CrossRef](#)] [[PubMed](#)]
33. Ma, L.; Liu, W.; Huang, Y.; Xian, G. Two acid sorbicillin analogues from saline lands-derived fungus *Trichoderma* sp. *J. Antibiot.* **2011**, *64*, 645–647. [[CrossRef](#)] [[PubMed](#)]
34. Jiang, C.-X.; Li, J.; Zhang, J.-M.; Jin, X.-J.; Yu, B.; Fang, J.-G.; Wu, Q.-X. Isolation, identification, and activity evaluation of chemical constituents from the soil fungus *Fusarium avenaceum* SF-1502 and endophytic fungus *Fusarium proliferatum* AF-04. *J. Agric. Food Chem.* **2019**, *67*, 1839–1846. [[CrossRef](#)] [[PubMed](#)]
35. Chen, Y.; Liu, Z.; Liu, H.; Pan, Y.; Li, J.; Liu, L.; She, Z. Anti-inflammatory activity from the mangrove endophytic fungus *Ascomycota* sp. CYSK-4. *Mar. Drugs* **2018**, *16*, 54. [[CrossRef](#)] [[PubMed](#)]

Sample Availability: Samples of all the compounds are available from the authors.



© 2019 by the authors. Licensee MDPI, Basel, Switzerland. This article is an open access article distributed under the terms and conditions of the Creative Commons Attribution (CC BY) license (<http://creativecommons.org/licenses/by/4.0/>).